Environmentally Controlled Fatigue Tests of Composite Box Beams with Built-in Flaws

J. D. Labor* and R. M. Verette†
Northrop Corporation Aircraft Group, Hawthorne, Calif.

Test results for two box beams are discussed in this paper. The beams had 32-ply graphite/epoxy tension skins that were 60 in. long by 18 in. wide. The graphite skins were mechanically attached to four aluminum spars and the compression skin was an aluminum "slave" skin. To explore the consequences of flaws and defects on structural performance, the box beams contained a variety of "built-in" flaws. Flaws included edge delaminations, surface scratches, foreign object damage, oversized holes, overtorqued fasteners, and delaminations at holes and through slots. The beams were tested in a wet condition, having been previously subjected to accelerated moisture conditioning. Fatigue testing involved two lifetimes of tension-dominated fatigue loading, representative of a typical fighter aircraft spectrum. Fatigue loading was followed by residual strength tests to failure. A major finding from the tests was that small-scale test results and analytical correlation based on small-scale tests can be used to predict the behavior of realistic aircraft composite structures.

Introduction

TO provide assurance that an aircraft composite structure will perform its function throughout its service life, it is necessary to move considerably beyond a demonstration that the static, dry, room temperature, unflawed strength is adequate. The real environment in which an aircraft operates consists of a complex spectrum of loading conditions. Because epoxy-based composites have an affinity for moisture, a realistic test condition must allow for absorption of moisture comparable to that which can occur during service. Repeated thermal cycles are also experienced by an aircraft during normal operations. Finally, real parts will eventually contain flaws, acquired either during manufacturing or during in-service use, and these should be considered in any test or analysis intended to show the adequacy of the structure. The need for tests of this type has been pointed out, for example, in Refs. 1 and 2.

This paper discusses fatigue tests of two panels tested as skins of box beam structures that dealt with several aspects of the real aircraft environment. In particular, the test panels were moisture conditioned prior to testing, were subjected to realistic random spectrum loading, and contained a variety of intentionally introduced flaws. Temperature excursions or effects were not addressed.

Although both of the panels tested contained flaws, the second panel also had built-in buffer strips to provide arrestment of damage. Both panels were tension skins made of AS/3501-5 graphite/epoxy. All other parts of the box beams were aluminum. Realistic structural details were used including flush-head mechanical fasteners. Numerous small-scale tests and analyses were conducted in support of the box beam tests.

Presented as Paper 77-475 at the AIAA Conference on Aircraft Composites: The Emerging Methodology for Structural Assurance, San Diego, Calif., March 24-25, 1977; submitted April 1, 1977; revision received Nov. 22, 1977.

Index categories: Structural Composite Materials; Structural Durability (including Fatigue and Fracture).

*Engineering Specialist, Structural Mechanics Research Department.

†Manager, Structural Mechanics Research Department. Member AIAA.

First Box Beam

Design and Fabrication

The test was configured as a box beam in which loads could be introduced to the test panel by both bending and torsion, to accurately represent a typical aircraft structure. Figure 1 shows an exploded view of a box beam, in which the test panel is the lower skin. The test panel was attached to four aluminum channel spars with 3/16-in. flush-head fasteners in clearance holes, with channel nut plates on the spar flanges. Tapered aluminum loading tabs were cold-bonded to the test panel and loaded by bolts through splice plates.

Torsion was applied at one end and reacted at the other to provide shear in the test panel, which caused load on the skin-to-spar fasteners. The four-point loading gave a constant bending moment over the central 5-ft test section.

Softening strips, in which zero-degree plies of graphite were replaced with zero-degree plies of E-glass, were used at all skin-to-spar fasteners. Preliminary design indicated that for this type of construction, both the fatigue stress allowable for the aluminum spars and the use of a matrix failure criterion for the graphite/epoxy skin would limit the strains at limit load so that softening of the holes would probably not be

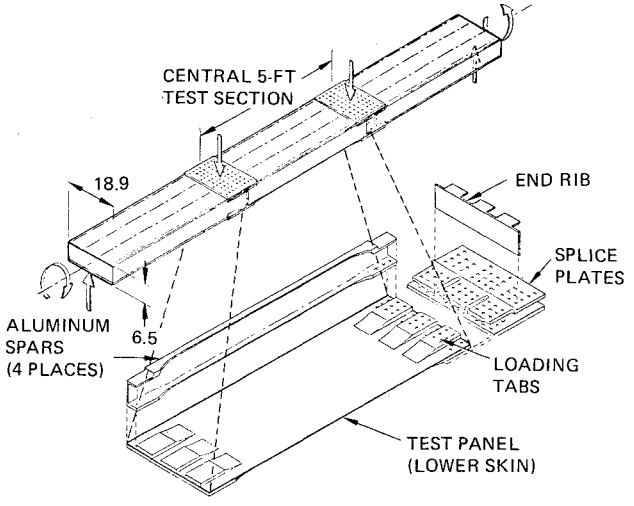

Fig. 1 Box beam loading fixture.

necessary. However, for the test specimen, the softening strips increased the strength at the holes so that flaws away from holes had a nearly equal probability of initiating failure.

The panel orientations used were

$$[\pm 45/0_3/90/0_4/90/0_3/\mp 45]_s$$

for the basic laminate and

$$[\pm 45/0_{2GL}/90/0_{3GL}/90/0_{2GL}/\mp 45]_s$$

at the softening strips, where the *GL* subscript denotes glass/epoxy plies.

At softening strips, 20 zero-degree plies of graphite were replaced by 14 zero-degree plies of E-glass, which resulted in a uniform thickness. No tapering of the graphite, spanwise or chordwise, was employed.

The flaws that were intentionally placed in the test panel are shown on the defect map in Fig. 2. Delaminations were simulated by embedding nonporous teflon-impregnated cloth between plies. At holes, the teflon disks were 0.6-in. in diameter. Vee-shaped surface scratches and foreign object damage (FOD) were created after the panel had been cured. Oversized holes had clearances five times as large as normal, and overtorqued fasteners were torqued to 75 in.-lb or to the onset of fiber damage on the countersunk side, whichever occurred first.

After the panel had been cured and loading tabs bonded, the tab area was painted to minimize corrosion of the aluminum tabs or degradation of the bondline. The skin-to-spar fastener holes were drilled slightly undersized in the central 30 in. of the panel in which the flaws were located. The panel was then moisture-conditioned by immersion in 180°F deionized water for 92 days. The moisture content was monitored by weighing small companion specimens cut from the same laminate. At the end of 92 days, the moisture content varied from 1.6 to 1.7%.

Testing

The panel was fabricated with extra width from which coupons were made to determine the laminate properties. The stiffness was found to be essentially identical to that of existing coupon data with no holes or flaws, whereas the tensile strength was 12% higher than the average of previous coupon values. Additional quality control tests verified the high quality of the panel. After moisture conditioning, the panel was strain gaged and installed in the box beam loading fixture.

Strain Survey

To evaluate the strain distribution across the width of the panel near each end, 18 strain gage rosettes were installed.

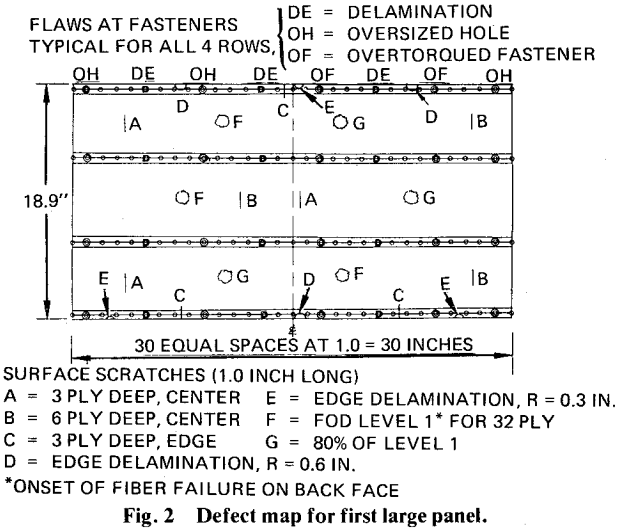

Fig. 2 Defect map for first large panel.

Strains were recorded for each leg of each gage for increasing loads for bending only, torsion only, and combined bending and torsion. The strain distribution across the width was observed to be quite uniform. Loads were applied up to 82.5% of the load at which matrix failure was predicted in the 90-deg plies of the basic laminate. The strain response was linear with increasing load and the distribution of the spanwise (0 deg) strain was uniform within approximately ±4% across the width. Shear stress was computed from the three-axis rosettes for the bending loading, and was negligibly small, indicating a uniform load introduction from the bonded tabs.

Strains were checked at 50% of maximum spectrum load during spectrum loading, and the strain survey for increasing loading was repeated at the completion of spectrum loading. No change in the magnitude or distribution pattern of strains was evident after spectrum loading.

Spectrum Loading

Loading conditions for the tension skin of the Northrop F-5 wing have been identified. For those loading conditions for which bending is large, the shearing load is typically small. For purposes of testing the box beams, the maximum bending condition was selected. This condition consists of a maximum axial load of 25,897 lb/in. Torsion was applied simultaneously with bending so that the maximum shearing stress in the test panel was 0.03468 times the tensile stress due to bending.

The same ratio of shear to tension was maintained during application of the tension-dominated spectrum loads. The loads are representative of those that would occur at the wing root of an air-superiority fighter aircraft. Approximately a half million loads constitute one lifetime. The maximum tensile stress in the spectrum was 33.2 ksi, which was established to prevent matrix failure. It occurred eight times during the two lifteimes of loading. This stress is 24% of the basic laminate strength and 36% of the strength of the basic laminate with an unflawed, softened hole, indicating that the resulting spectrum is relatively mild loading for this laminate. The spectrum rms stress was 4.417 ksi. The spectrum does contain a relatively few number of compressive loads of low magnitude that occur on the wing tension surface. The maximum compressive stress was −7.46 ksi. It occurred four times during the two lifetimes of loading.

Approximately two and a half weeks of around-the-clock testing with a loading cycle applied about every 3 seconds, were required to simulate two lifetimes of fatigue loading. The panel was visually examined before spectrum loading, again after one lifetime, and again after two lifetimes. No damage was observed and no loosening of fasteners had occurred. To maintain moisture content during spectrum loading, water was added to felt pads laid between spars against the panel on the inside of the box beam, and the entire central 5-ft test section was wrapped in plastic. The moisture content was determined by weighing companion specimens which remained with the panel during testing. Variation during spectrum loading was from 1.6% at the start to 1.7% at the end of two lifetimes and 1.68% at static failure.

Static Loading to Failure

The load at which panel failure was predicted to occur was computed based on existing coupon data as described later, and this load was defined as 100%. During loading, torsion was applied to cause shear stress as a constant fraction of bending stress in the same proportions as described above for spectrum loading.

Loads were applied at approximately 10% per min, with 10 second pauses for strain gage recording at 10% intervals up to 80% and at 5% intervals above 80%. Safety considerations precluded close visual examination during loading, but from several feet away no damage was observed prior to failure. Sounds that were probably matrix cracking and possible delamination became audible above 85% load.

At 95% load, failure occurred suddenly and catastrophically. The full width of the graphite test panel broke and three of the four aluminum spars failed at the lower flange with the web tearing up to the upper flange. The upper aluminum slave skin was bent but otherwise undamaged. Splice plates and ribs at the ends of the 5-ft test section were not damaged.

Although the point at which failure initiated is not obvious, several detailed aspects of the failure zone are described below.

1) Much of the failure zone follows a line at 45 deg to the span direction, as shown in Fig. 3, indicating that shearing stresses became significant in the panel during the failure sequence. Two sources contribute to this: a) the small shear due to torsion became much larger as part of the skin panel failed so that the effective torque box was reduced; and b) as part of the panel failed, the bending load sheared laterally to the stiffer, unbroken part of the panel.

2) Considerable local damage exists at fastener holes adjacent to the break, as shown in Fig. 3. After disassembly, these holes showed local crushing due to fasteners bearing against the panel toward the break. This suggests that after the panel failed, the load in the panel was transferred through the fasteners to the spar until the spar failed.

3) The failure zone passed through a six-ply-deep surface scratch as shown in Fig. 3. The top six plies delaminated, and the failure line for the remaining plies ran straight by the area at a 45-deg angle, indicating that the scratch did not initiate failure, but was merely in the path of the failure zone that started elsewhere.

4) A triangular portion of the panel was displaced laterally, as shown in Fig. 3. The spar flange split longitudinally through the fasteners and the spar displaced laterally approximately ½ in. The heel of the flange and the web were not fractured. The lower flanges of the other three spars were broken and their webs were torn for their full depths.

5) Areas at the tips of loading tabs lifted off with part of the top 45-deg ply of graphite adhering to the tab. This occured only on the tabs at the end of the panel near the failure on both the inside and outside of the panel, and only between the two central spars. This intralaminar failure extended ½-¾ in. back from the tip of the tab, indicating that the load introduction peaked in the center bay between spars during failure, suggesting that the failure probably started in one of the outer bays.

6) Along most of the failure line, delamination was confined to an area within ½ in. on each side of the break, except for some surface fiber separation. However, the separated triangular piece of the panel contained multiple delaminations through the thickness.

Relative Severity of Flaws

A comparison of the relative severity of each of the flaws in the first box beam panel is shown in Table 1. The percent of the unflawed laminate strength that remains for each type of flaw is shown. These percentages were obtained from small-scale tests discussed in Ref. 3. The flaws away from holes are consistently less damaging than unflawed or flawed holes, and so failure is expected to initiate at one of the fasteners. Based on existing coupon test results for unloaded holes (Ref. 3), the overtorqued fasteners resulted in the lowest strength at 61.0% of the unflawed laminate strength. This value is only slightly less than the 66.8% strength for an unflawed hole. This indicates that the effect of the flaws at holes that were tested is small, and that the specific hole at which failure initiates may be influenced more by minor variations in the stress distribution than by the presence of specific flaws. The loaded softened hole data of Table 1 were for holes loaded much more heavily than those in the first box beam, and hence the unloaded fastener coupon data are more applicable.

Analysis of Static Failure

The relative severity of the various flaws placed in the test panel was determined by comparison of coupon test results and has been summarized in Table 1. These data indicate only small differences between the strengths for an unflawed hole and for holes with the various flaws present. However, for the purpose of predicting the strength of the large-scale panel, the most severe condition was used, i.e., a hole with an unloaded overtorqued fastener for which 61.0% of the "no-hole"

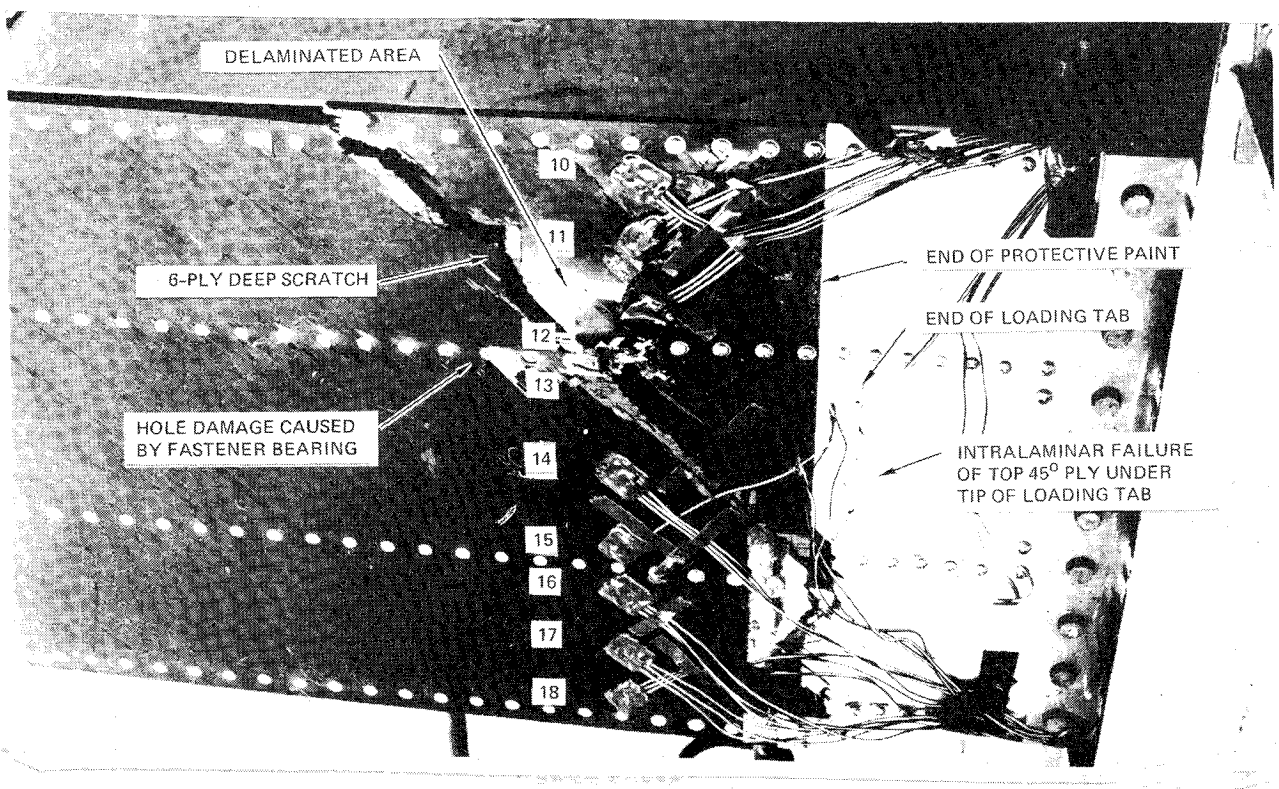

Fig. 3 First large panel after failure.

Table 1 Strength reduction due to flaws in first box beam

Flaw	% of basic laminate tensile strength
Center scratch: 3 plies deep	75.1
6 plies deep	69.7
Edge scratch: 3 plies deep	75.1
Edge delamination: $R=0.6$	103.0
$R=0.3$	105.9
FOD: level F (Fig. 2)	74.5
80% of F	...
Unloaded softened holes	
No flaw	66.8
Delamination at hole	70.7
Overtorqued fastener	61.0
Oversized hole	...
Loaded softened holes	
During spectrum only	
No flaw	72.3
Delamination at hole	62.5
Overtorqued fastener	71.4
Oversized hole	...
During static only	
No flaw	44.6
Oversized hole	54.1
During spectrum and residual	
Oversized hole	46.8

laminate strength remained. This is based on an average coupon strength of 81.3 ksi in the graphite material, computed using an effective area which accounts for the reduced stiffness of the E-glass softening strip material. For the predicted failure stress of 81.3 ksi and the bending moment of inertia of the box beam computed from drawing dimensions, the predicted bending moment at failure was 2.12×10^6 in.-lb, and this value was subsequently defined as 100% load. The computed moment of inertia at midspan accounted for the varying stiffnesses of the graphite panel, the E-glass softening strips, and the aluminum spars and slave skin.

Failure of the panel occurred at 95% of the predicted failing load. The test procedure and a description of the failure zone were given previously.

The ability to predict the load at failure within 5% lends considerable confidence to the direct use of small-coupon test data for analysis of large-scale structures. However, a number of conditions existed that may have affected the panel strength, some of which would tend to reduce the strength, whereas others tend to increase it. The excellent correlation between predicted and actual failure loads is probably the result of these effects tending to offset each other.

Although most of the effects cannot be evaluated quantitatively, certain trends can be recognized. These would be important to consider in the planning of tests to be used for the qualification of specific composite components for future applications.

Conditions that tend to cause failure at less than the predicted load are discussed below.

1) *Fastener Loading.* Predicted failure was based on unloaded fastener coupon data. Because of the small torsion applied to the box beam, small shear stresses existed in the panel. Based on finite-element analysis of loaded fasteners, the fastener loads on the larger panel are approximately 1/7th as severe as the fastener loads on coupons used to develop the loaded hole data of Table 1. Although specific data for this lighter loading are not available, some small reduction in strength may have resulted from the light fastener loading.

2) *Edge Effects.* The coupon strength data of Table 1, on which the large-panel predicted strength was based, were for 2-in.-wide specimens with fasteners centered in a softened strip 0.75 in. wide with parent laminate on each side of it. The fasteners in the edge spars of the large scale panel are in the softened strip extending to the edge of the panel. Some reduction in strength probably exists because of this effect and suggests that the large panel failure may have initiated at edge fasteners.

3) *Substructure.* The flaws introduced in the central 30 in. of the test panel were not appreciably more severe than plain holes that existed over the full length of the panel. As a result, failure was not forced to occur near midspan. Geometric changes in the cross section at the ends of the spars and at the splice plates may have shifted the bending neutral axis to change the effective moment of inertia and the distance to the panel. Since failure did occur toward one end of the panel, it is likely that the effect of the substructure tended to cause failure at a slightly reduced load from that predicted.

4) *Strain Distribution.* As discussed above, the distribution of strains across the width of the panel was considered very uniform, varying by only a few percent. Since the implanted flaws did not force failure near the center, a portion of the failure occurred between the loading tabs and the strain gages. The strain distribution near the tabs may have been less uniform with peak strains tending to initiate failure at lower loads than were predicted.

5) *Moisture Conditioning.* The moisture content of the large panel was slightly less than the moisture content of the coupons, i.e., 1.68 vs 1.8%. It is doubtful that this small difference had any effect on a fiber-controlled failure. However, because the large panel was 32 plies thick compared to 16 plies for the coupons, it had been immersed 92 days compared to 60 days for coupons to gain adequate moisture. It is possible that the length of immersion time may effect strength, especially when matrix or interface strength loss with E-glass softening strips can contribute to delamination or local failure at stress concentrations.

6) *Scale Factor Effects.* Because a large panel contains more material than a small coupon, it has a higher probability of containing a weak spot that might initiate failure. This effect would be expected to be less significant when the potential failure sites are limited to a finite number of fastener holes than for an unflawed laminate. However, the larger size of the panel tends to reduce the probable load at which failure initiates.

Conditions that tend to cause failure at higher than the predicted load are discussed below.

1) *Basic Laminate Strength.* Coupons cut from the laminate adjacent to the larger panel showed a static tensile strength 12% higher than the average for the basic laminate material properties as determined by coupon data in Ref. 3. This and acid-digestion physical property evaluation both indicate that the large-scale panel was of generally high quality. No unflawed, unholed strength data are directly available for the material from which the coupons with holes were made and from which failure loads were predicted. Therefore a direct evaluation of the effect of the quality of the large panel is not possible. A tendency toward slightly higher than average strength must be considered as a possible effect on the actual load at failure.

2) *Location of Failure.* The predicted failing load was based on the coupon strength for overtorqued fasteners, for which 61.0% of the basic laminate strength remained, as compared to 66.8% remaining for an unflawed hole. Since the failure zone did not include an over-torqued fastener location, a tendency toward a higher load at failure must be considered.

Second Box Beam

Design and Fabrication

The box beam loading arrangement described above for the first panel was used for the second panel. New spars and a new slave skin were installed to replace those damaged during the first box beam test.

The second panel was nearly identical to the first panel, except for the addition of buffer strips and a different pattern of flaws. The same laminate was used with the following

orientations: $[\pm 45/0_3/90/0_4/90/0_3/\mp 45]_s$ for the basic laminate and $[\pm 45/0_{3GL}/90/0_{4GL}/90/0_{3GL}/\mp 45]_s$ at the longitudinal buffer strips. That is, where buffer strips were installed, the 0-deg graphite plies were replaced, ply for ply, by 0-deg E-glass/epoxy strips. Buffer strips, ¾ in. wide, were located at each of the four spars and at three locations centered between spars, making the seven buffer strips at approximately 3-in. spacing. Transverse buffer strips, in which only the 90-deg plies of the basic laminate were replaced by ¾ in. E-glass strips, were spaced at 3 in. At the intersection of the 0-deg and 90-deg buffer strips, the greater thickness of the E-glass plies combined to create a slightly increased thickness. To provide a flat surface against the spars, the longitudinal 0-deg buffer strips at the spars had fillers consisting of two plies of 90-deg graphite/epoxy added at the mid-thickness of the panel.

The buffer strip pattern and the flaws that were intentionally placed in the panel are shown in Fig. 4. Of all the flaws shown, three types, viz., surface scratches, through slots, and impact damage, had previously been investigated specifically using small panels with buffer strips. The other flaws were investigated for panels without buffer strips and were included on the first large panel. To provide continuity with the first panel, these other flaws were included in the second large-scale article. The flaw locations were selected to provide a uniform distribution of flaws. The more severe flaws (through slots and impact damage) were spaced apart by at least two rows of buffer strips to minimize their influence on each other during crack initiation and after crack arrestment. The most severe flaw, which was expected to govern cracking, arrestment, and ultimate failure, was a 2-in. long through slot toward the left end of the test section.

After flaws were created and the fastener holes in the central 30 in. of the panel were drilled slightly undersize, the panel was moisture conditioned by immersion in 180°F deionized water for 102 days. The moisture content, determined by weighing small coupons cut from the same laminate, was approximately 1.7% by weight and varied from that only slightly during testing.

Testing

The second panel was assembled into the box beam loading fixture that had been used for the first panel test. New spars and a new slave skin were installed to replace those damaged in the previous test. Strain gage rosettes were installed as shown in Fig. 5, each gage centered between buffer strips. Gage number 7 was located in line with the 2-in.-long through slot and 3.5 in from it as shown. Because of the less stiff load path in line with the slot, gage number 7 consistently measured a lower strain than the average, while gages 6 and 8 on each side of it read higher than average. The spanwise strain distribution across each end of the panel before and after spectrum loading is shown in Fig. 6. Based on strain gage readings, the maximum spectrum load was scaled to give a stress level of 33.2 ksi in the graphite/epoxy panel.

Very early in the first lifetime, surface cracks approximately ¼ in. long were found extending from the ends of the critical 2-in.-long slot. Strain gage readings at this time indicated a significant softening in the area of the slot. During the balance of the spectrum loading, the surface cracks grew well into the buffer strips. This had been expected based on the similar behavior observed for small panels with buffer strips that had been exposed to spectrum loading. By the end

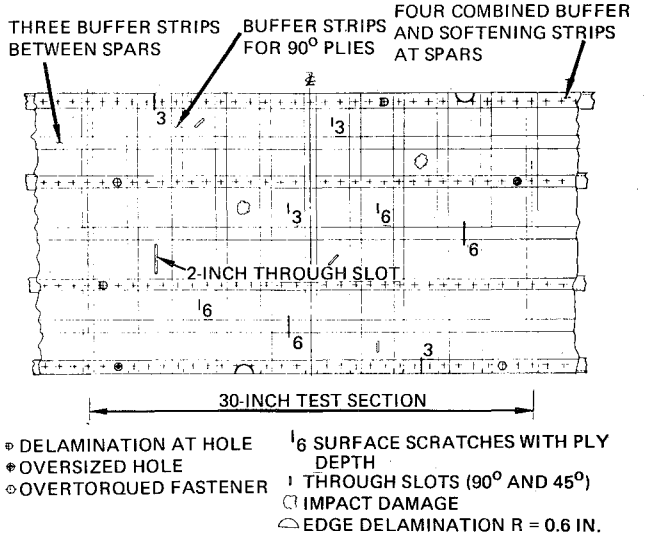

Fig. 4 Defect map for second large panel.

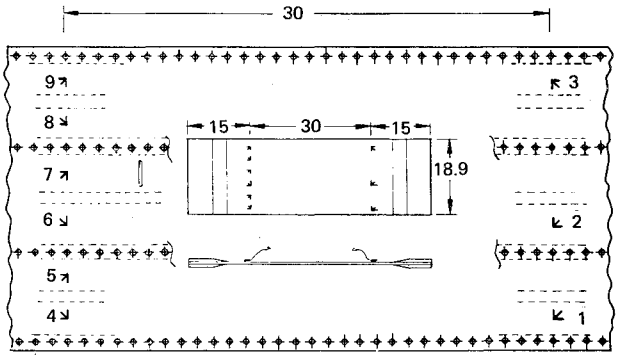

Fig. 5 Strain rosettes on second large-scale panel.

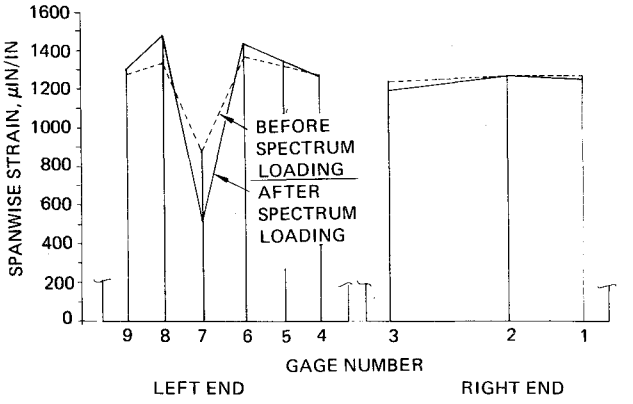

Fig. 6 Strain distribution at 50% of maximum spectrum load.

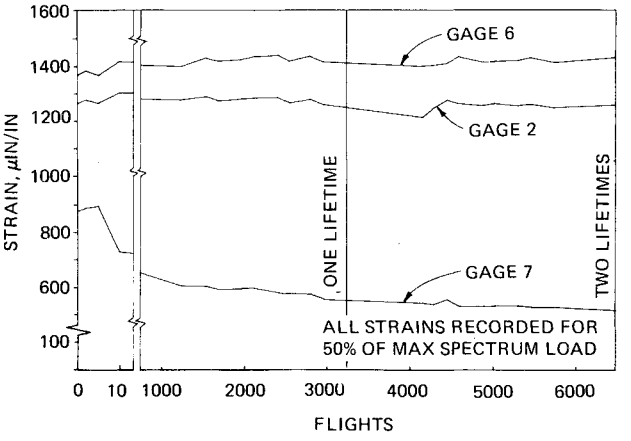

Fig. 7 Second large panel strains during specimen loading.

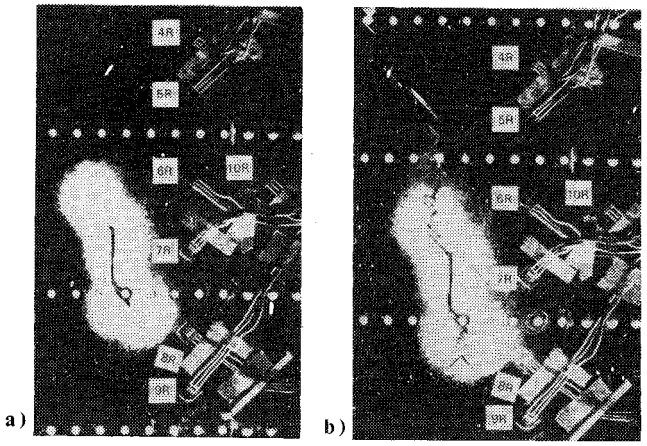

Fig. 8 Initial failure of large-scale panel with buffer strips: a) before initial failure; b) after initial failure.

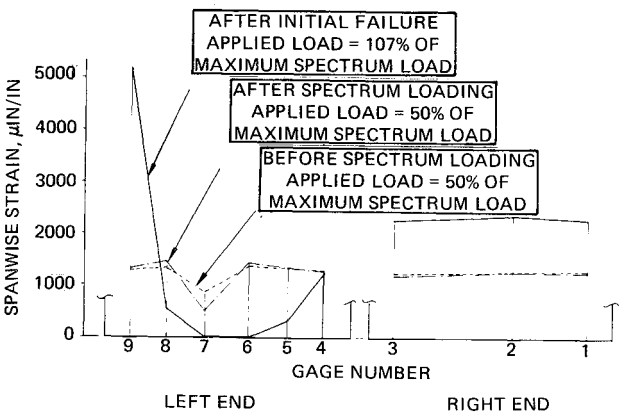

Fig. 9 Strain distribution after initial failure.

of two lifteimes the surface cracks at one end of the slot were up to ¾ in. long. At the other end of the slot adjacent to the spar, the surface cracks had grown into a fastener hole and about ½ in. on beyond the hole. Acoustic nondestructive inspection indicated a delaminated area in the buffer strips at both ends of the slot.

The changes in spanwise strain gage readings during spectrum loading are shown for three gages in Fig. 7. Gage number 7, in line with the slot, shows a significant drop in strain between five and ten flights and then shows a gradual decrease in strain during the remainder of two lifetimes. The correlation between the observed increase in surface cracks and this decrease in strain is significant to the growth and arrestment of damage during spectrum loading.

The residual strength of the panel with arrested cracks was predicted using small-panel test data as described below. The loading to produce the predicted stress in the graphite panel at failure, 39.5 ksi, was 119% of maximum spectrum load, with a possible scatter of ±10-15%. During static loading, strains increased linearly with load for all gages, including gage number 7 at the slot.

At 107% of maximum spectrum load, initial failure occurred after the load had been held for approximately 5 seconds while gages were read. Initial failure was sudden with no visible extension of surface cracks prior to failure. The panel initially broke from only one end of the slot. Figure 8a shows the surface cracks before initial failure in which the cracks appear the same as they did at the end of spectrum loading. The photograph in Fig. 8b shows the initial failure from one end of the notch to the edge of the panel, but only slight crack entension from the other end of the notch.

After a slight load drop, the hydraulic system returned the load to the 107% level and this load was held for approximately 1 min. As a result of this initial failure, the midspan deflection increased from 1.87 in. to 2.50 in. The distribution of spanwise strain, after this initial failure with 107% of maximum spectrum load applied, is shown in Fig. 9. For comparison, the distributions before and after spectrum loading are also shown for 50% of maximum spectrum load.

The strain distribution after initial failure indicates that although no load was carried through the central failed area of the panel around the crack, both edges of the panel, i.e., near gages 9 and 4, were carrying load. The panel at gage 9 appeared unfailed and most of the load was carried in that area as indicated by the high strain at gage 9. However, a significant strain remained at gage 4, indicating that some load was carried at that edge of the panel in spite of surface cracks. It appears that the buffer strips near gage 4 partially arrested the damage and prevented failure of some of the internal plies so that a load path remained even with surface plies broken. As shown in Fig. 9, the strains at the right end, away from the failure, remained uniform across the width. After the 107% load level had been held for approximately 1 min and with the load still held constant, the balance of the panel failed.

Correlation with Small-Panel Data

The large-scale panel test successfully demonstrated that the crack arrestment behavior and strength of small-scale panels with buffer strips are good indications of the behavior and strength of large, realistic aircraft-type skin panels. A limited number of small-panel tests were directly applicable to the configuration used for the large panel. The small-panel tests applicable to the large panel are listed in Table 2 (Ref. 3).

From the data in Table 2, it is apparent that surface cracks initiated during spectrum load exposure for every spectrum-exposed panel except MS1-2, and after completion of spectrum loading, surface cracks initiated in it during static loading, at a stress less than the maximum spectrum stress. At the end of spectrum loading the length of visible surface cracks varied from ¼ in. to about 1.5 in. long, always at 45 deg to the load direction, i.e., matrix cracks appeared between fibers of the surface ply. This visible surface cracking also occurred on the large panel early in the spectrum loading as had been expected from the small-panel behavior.

As shown in Table 2, arrestment occurred for cracks that initiated during spectrum loading for all panels except UF 7-3 which failed during spectrum loading. Based on these results, arrestment and successful completion of two lifetimes of spectrum loading were expected for the large panel, and as previously described, the two lifetimes were completed.

Stress levels at ultimate failure are shown in Table 2 for the small panels. All stresses are based on an effective area that allows for the different stiffnesses of the basic laminate and the buffer strip hybrid material. The stresses shown are the actual stresses in the basic laminate at failure. The lowest stress is 30.0 ksi and the highest value shown is 48.0 ksi for static testing of panel UF4-1. This wide variation in stress level does not correlate with either the number of buffer strips or with the absence or presence of spectrum loading. The stress at failure is believed to depend primarily on the amount of damage (surface ply cracks, interior ply cracks, and delamination) that occurs prior to failure, and the amount of damage appears to vary widely among the panels tested.

With the large variation in small-panel stresses at failure, it was difficult to use the data to predict failure loads for the large panel. Since small panel MS2-3 was most representative of the large panel, i.e., it had spectrum load exposure and it had fastener holes adjacent to the notch, and because its stress at failure, 39.5 ksi, is in the mid-range of the failure stresses for all the panels, its stress, 39.5 ksi, was selected as the most likely stress at failure for the large panel. The load to produce this stress in the basic laminate, using the effective area of the large panel, was 119% of maximum spectrum load. Failure occurred at 107% of maximum spectrum load, or at a stress

Table 2 Test results – small panels with buffer strips

Specimen number[a]	No. of buffer strips	Static or spectrum	Stress at initial cracking, ksi	Crack growth mode	Arrested	Stress at ultimate failure, ksi
UF4-1	2	Static	31.1	Slow	Yes	48.0
UF4-3	2	Spectrum post-arrest	31.6	Slow	Yes	46.0
UF7-1	2	Spectrum	During spectrum	Slow	Yes	35.8
UF7-2	2	Spectrum	During spectrum	Slow	Yes	30.0
UF7-3	2	Spectrum	Failed during spectrum loading			
MS1-1	4	Spectrum	During spectrum	Slow	Yes	35.46
MS1-2	4	Spectrum	32.3	Slow during static load	[b]	42.6
MS1-3	4	Spectrum	During spectrum	Slow	Yes	43.9
MS2-3	5[c]	Spectrum	During spectrum	Slow	Yes	39.5
MS2-2	5[c]	Static	24.1	Slow	[b]	35.0

[a] All panels are $[\pm 45/0_2/90/0_3]_S$, moisture conditioned (1.8%), with 2-in.-long through slot centered between buffer strips.
[b] Visible surface cracks continued to grow into buffer strips as load increased to failure.
[c] Panels MS2-3 and MS2-2 had countersunk 3/16 fastener holes adjacent to one end of slot, no fastener installed.

level of 35.5 ksi, which is within the scatter of the small-panel data. Since rather extensive damage was observed in the large panel after spectrum loading, it is not surprising that failure occurred at a slightly lower stress level than predicted.

Conclusions and Recommendations

The results of the two large-scale tests indicate that composite coupon strength data can be used to predict the strength of large aircraft components with a degree of precision that is well within the scatter of typical test data. The severity of flaws in reducing the strength of a laminate can be adequately assessed from small-scale tests. The theoretical effect of specimen size based on the higher probability of larger specimens containing more weak spots becomes of minor importance when the potential failure sites are constrained to a finite number such as at specific fastener holes.

The accuracy of predictions based on coupon data will be influenced by minor differences between the coupons and the actual component, and so these differences should be minimized. Geometrical differences including edge effects, fastener hole tolerances, method of load introduction, and laminate thickness need to be accurately simulated in coupons. The normal scatter in basic laminate strength must be adequately evaluated and considered in establishing a range of strength values based on probability. Although the effects of moisture have yet to be fully evaluated, the test data for coupons and the large-scale panels were based on moisture contents which are probably higher than would be realized in actual service. As a result, moisture effects have been accounted for in a conservative manner.

Only a single load condition could be carried to failure, and failure could initiate at only one location in each panel. Therefore, the success of these tests is limited to the geometry and loading conditions used. Additional testing of this type with more severe spectrum loading, more severe flaws, other loading conditions, and other laminate configurations would be desirable to fully demonstrate in detail the correlation between the strengths of coupons and large panels.

The second large-scale panel test successfully demonstrated three aspects of crack arrestment behavior that were predicted based on the small panel data:

1) Development of damage, as evidenced by visual cracks between fibers of the surface ply, was expected and did occur in the large panel during spectrum loading.
2) Arrestment of the damage and completion of two lifetimes of spectrum loading was expected, and was accomplished for the large panel.
3) The ultimate failure stress in the large panel was within the range of failure stresses obtained from small panels.

In addition to the successful arrestment of damage during spectrum loading, the potential value of buffer strips was further demonstrated in that after a severe initial failure, the load was held for approximately 1 min before complete failure occurred. This delay in complete failure could save an aircraft which had experienced a structural failure during a brief high load maneuver and permit a safe return to its base.

Acknowledgment

This work was accomplished as a part of Contract F33615-74-C-5182, "Structural Criteria for Advanced Composites." E. Demuts, AFFDL/FBC, was the project monitor.

References

[1] Goodman, J. W., Lincoln, J. W., and Bennett, T. H., "The Air Force Structural Integrity Program for Advanced Composite Structures," *AIAA Conference on Aircraft Composites: The Emerging Methodology for Structural Assurance, Volume A of Conference Papers*, March 1977, pp. 381-387.

[2] Weinberger, R. A., Somoroff, A. R., and Riley, B. L., "U.S. Navy Certification of Composite Wings for the F-18 and Advanced Carrier Aircraft," *AIAA Conference on Aircraft Composites: The Emerging Methodology for Structural Assurance, Volume A of Conference Papers*, March 1977, pp. 396-407.

[3] Verette, R. M. and Labor, J. D., "Structural Criteria for Advanced Composites," AFFDL-TR-76-142, Vol. I, March 1977.